STARRO

WHITE PAPER | THERMAL | REVISION 2

Contained Cell Failures for Battery Pack Engineers

Thermal-runaway propagation in a potted 12-cell 21700 module, with and without 1.5 mm aerogel sleeves: a transient 3D conduction model with stated inputs, checks and sensitivities.

Published
November 2026

Method
Transient 3D finite-volume conduction

Authors
Starro Research Team

Abstract

One cell in a potted module of twelve 21700 cells is forced into thermal runaway with an 85 kJ total heat release. With conductive potting alone, the hottest neighbor-cell wall reaches 224 °C at 38 s and stays above the 185 °C critical temperature measured for NMC-811 21700 cells [2] from 20 to 86 s. With 1.5 mm aerogel sleeves and the vent gas ducted away, the peak is 84 °C at 190 s, below the 101 °C self-heating onset [2].

The sleeves interrupt the lateral path only. With about 24 % (9 kJ) of the vent heat deposited on the lid, or with the lid in contact with the cell tops (128 °C), the sleeved neighbor exceeds the self-heating onset. With the three least favorable lateral inputs combined it reaches 110 °C. Sleeves are effective but have little margin unless the top of the module is designed as part of the barrier.

Keywords: battery thermal runaway, propagation, 21700 cell, aerogel sleeve, potting, battery pack design

1. Introduction

In a tightly packed module, a cell in thermal runaway can heat its neighbors past their own runaway threshold. Feng et al. tested six 25 Ah NCM batteries, each two pouch cells in an aluminum shell, clamped face to face; heat conducted through the shells dominated propagation, and about 12 % of one battery's runaway heat was enough to trigger the next [1]. Potting compounds that improve normal-operation cooling strengthen this lateral path in cylindrical-cell modules. This study asks whether 1.5 mm aerogel sleeves stop lateral propagation in a potted 21700 module, and where they stop working.

2. Model and Method

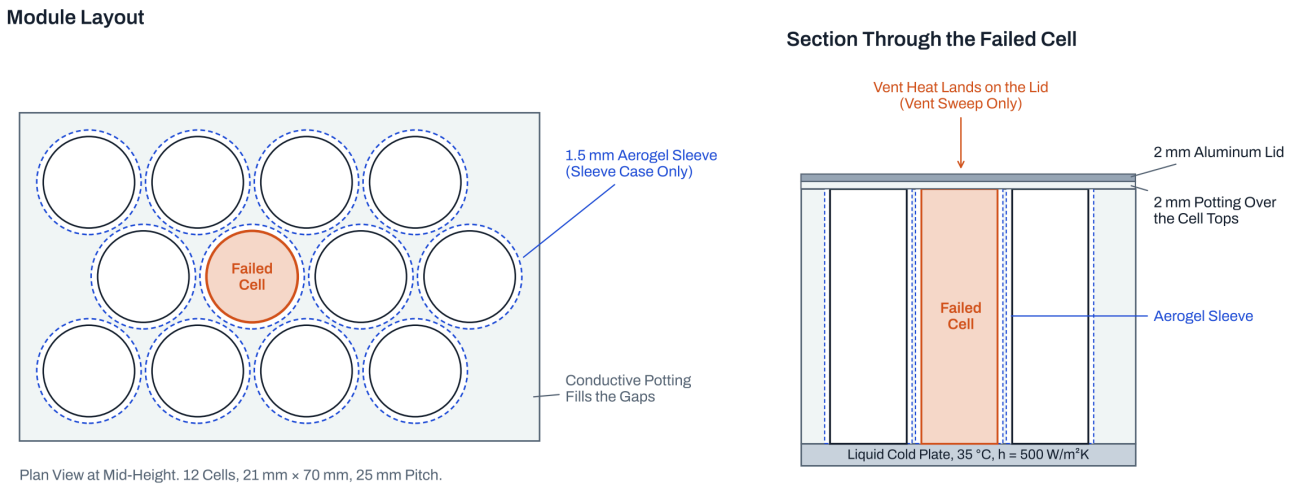


Figure 1. Module layout (plan to scale) and section through the failed cell (schematic). Dashed outlines: aerogel sleeves, present only in the sleeve design.

2.1 Geometry

Twelve 21700 cells (21 mm × 70 mm) in three staggered rows of four at 25 mm pitch, with a 4 mm potting wall beyond the outer cells. Potting fills the inter-cell space and forms a 2 mm layer over the cell tops; a 2 mm aluminum lid covers the module. The cell bottoms sit on the cold-plate boundary. In the sleeve design each cell carries a 1.5 mm aerogel annulus over its full height. The failed cell is the second cell of the middle row, which has six neighbors.

2.2 Physics

Transient heat conduction,

$$\rho c_p \, \partial T/\partial t = \nabla\cdot(\mathbf{k}\nabla T) + q'''(t),$$

with anisotropic conductivity in the neighbor cells. The failed cell releases Q_{body} = 44.7 kJ into its own volume at rate $q(t) = Q\, t/\tau^2\, e^{-t/\tau}$, τ = 3 s (85 % by 10 s). A further 40.3 kJ leaves with the vent gas, for a total of 85.0 kJ. NASA fractional thermal runaway calorimetry measured average totals of 82.5 to 85.8 kJ for 5 Ah 21700 cells triggered by heaters, and up to 98.3 kJ by nail penetration [3]. Retained entirely, 44.7 kJ would take the failed cell to 666 °C; the peak surface temperature measured on this cell type in accelerating rate calorimetry is 571 to 613 °C [2], which is consistent with this body share. In the vent sweep a fraction f of the vent heat is deposited uniformly on the lid within 20 mm of the failed-cell axis, with the same time profile.

2.3 Failed Cell

During runaway, decomposition, gas generation and internal shorting redistribute heat inside the cell much faster than intact radial conduction would. We treat the failed cell as near-isothermal (isotropic k = 50 W/m·K). Its modeled mean temperature peaks at 437 °C with potting and 595 °C with sleeves, consistent with the 571 to 613 °C peak measured in accelerating rate calorimetry [2]. A run with intact-cell conductivity is included in the sensitivities.

2.4 Boundary and Initial Conditions

Uniform 35 °C at t = 0. Bottom face: h = 500 W/m²·K to 35 °C coolant (liquid cold plate and interface). Top face: h = 10 W/m²·K to 35 °C. Side walls adiabatic.

Material	k (W/m·K)	ρ	c_p (J/kg·K)	Source
Cell, radial / axial	0.20 / 30	mass-matched	1100	k: Drake et al. via [4] (18650 and 26650 cells); c_p assumed
Failed cell during runaway	50	mass-matched	1100	Lumped assumption (see text)
Steel can, 0.25 mm	40 equiv.	mass-matched	500	One grid ring; k scaled to preserve conductance
Conductive potting	1.5	2200	1000	Typical filled potting; assumed
Aerogel sleeve	0.046	200	1000	Pyrogel XTE at 400 °C mean [5]; c_p assumed
Aluminum lid (6061)	167	2700	896	Handbook values

Table 1. Material inputs, constant with temperature. Mass-matched: each voxelized core and can carries exactly 60.3 g and 9.0 g, so every cell weighs 69.3 g [2] on every grid. The aerogel value is the datasheet conductivity at 400 °C mean temperature, close to the mean temperature of the sleeve around the failed cell; 28 and 64 mW/m·K (200 and 500 °C) are run as sensitivities [5].

2.5 Failure Criteria

The maximum temperature of any neighbor-cell wall is compared with values measured by accelerating rate calorimetry on NMC-811 21700 cells at 100 % state of charge [2]: self-heating onset T_1 = 101.4 to 102.6 °C (heating rate above 0.001 °C/s), venting T_v = 115.8 to 127.3 °C, and critical self-heating temperature T_2 = 184.7 to 186.0 °C (about 0.33 °C/s, after Ohneseit et al.). These are whole-cell values; a hot wall with a cooler interior is a local condition. We report the time the wall spends above each value and the neighbor's bulk mean. The polyethylene separator in cells of this type melts at about 130 to 140 °C [6]; this is the likely mechanism by which a hot can wall starts a local internal short, though the ceramic coating used on such separators can delay it.

2.6 Numerics

Cell-centered finite volumes on a voxel grid, 0.75 mm in plane and 5 mm vertically (254,400 cells), harmonic-mean face conductances, backward-Euler time integration (Δt = 0.5 s to 40 s, 1 s to 120 s, 2 s after), algebraic-multigrid-preconditioned conjugate gradients to a relative residual of 10^{-8}. All runs cover 300 s except the vent cases at 35 % and above and the fine-grid potting check (150 s); vent-case peaks occur by 20 s, but for 50 % and above the wall is still above T_1 at 150 s, so time above T_1 is not resolved for those cases. The model script, run scripts and outputs are retained with this paper.

3. Results

3.1 Lateral Propagation

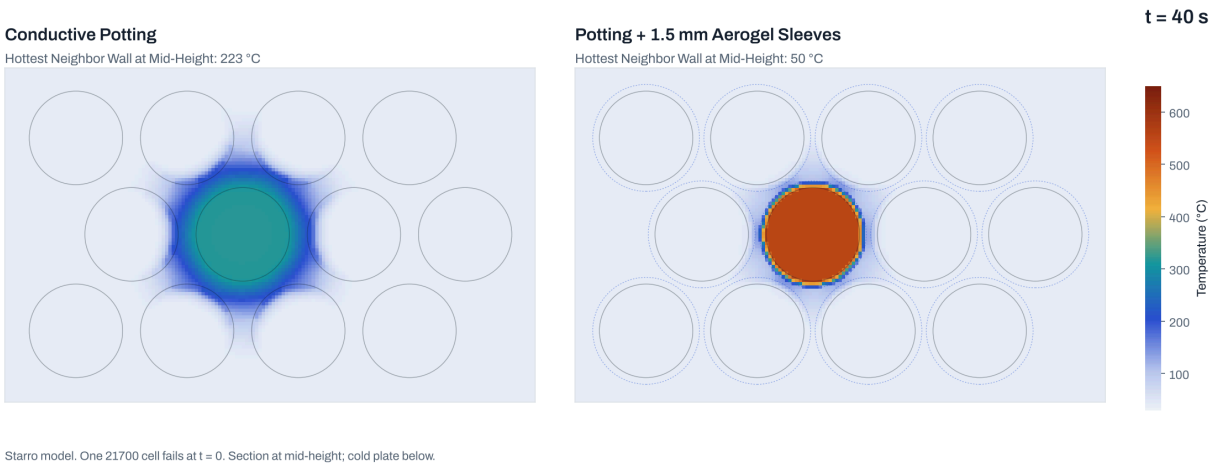


Figure 2. Temperature at mid-height, 40 s after failure. Left: potting only. Right: potting with aerogel sleeves. Same scale. The web version animates the first 120 s.

Quantity	Potting Only	Aerogel Sleeves
Peak neighbor-wall temperature	224 °C at 38 s	84 °C at 190 s
Wall above T_1 (101 °C)	11 to 234 s	never
Wall above T_2 (185 °C)	20 to 86 s	never
Peak neighbor bulk mean	61 °C	54 °C
Peak failed-cell mean	437 °C	595 °C

Table 2. Base-case results (vent gas ducted away; no heat on the lid).

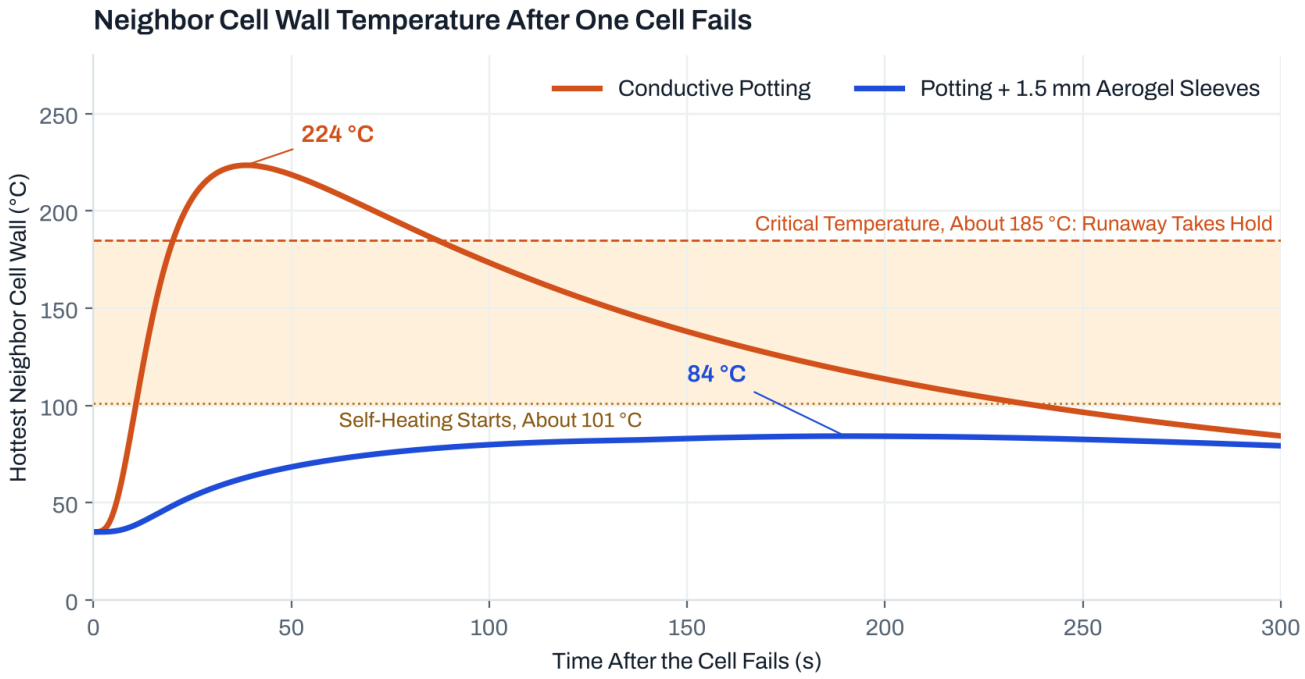


Figure 3. Hottest neighbor-cell wall temperature. Shaded: between T_1 and T_2.

With potting alone the neighbor wall exceeds T_2 for about 66 s near mid-height while the neighbor's bulk mean stays at 61 °C: the likely failure mechanism is a hot wall causing a local separator breach rather than whole-cell heating, although ceramic-coated separators can delay the short. With sleeves the failed cell retains its heat (mean 595 °C, consistent with the measured peak) and the neighbor wall rises slowly to its peak in the upper half of the cell, fed by leakage through the sleeve and the 2 mm potting layer over the cell tops.

3.2 Heat From Above

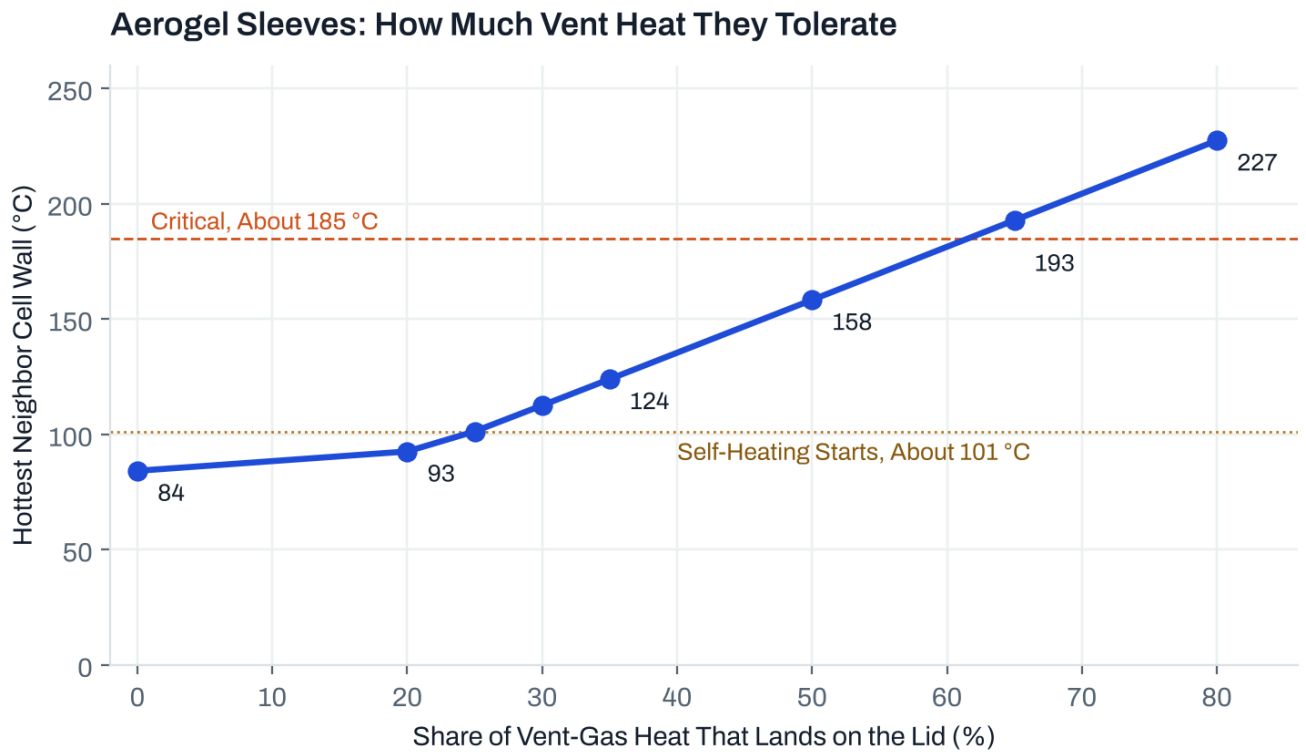


Figure 4. Sleeve design: peak neighbor-wall temperature against the fraction of the 40.3 kJ vent heat deposited on the lid.

With no vent heat on the lid, the neighbor stays at 84 °C. With about 24 % of the vent heat on the lid (roughly 9 kJ), the top of the neighbor cell passes 101 °C, the measured self-heating onset. Near 60 %, it passes 185 °C. At 80 %, it reaches 227 °C. From 25 % up, the neighbor peaks within about 20 seconds, because the heat comes straight down from the lid. Deposition above about 30 % also exceeds T_v, so the neighbor may vent. With the lid in direct contact with the cell tops and no vent deposition, the neighbor reaches 128 °C; busbars form a similar metallic top path and are not modeled.

4. Verification

Check	Result
Energy bookkeeping (released = stored + lost)	Error below 10^{-6} in every run (confirms solver consistency, not accuracy)
Adiabatic limit	Failed-cell mean below its own adiabatic limit in every run
Time step halved	Peak changes 0.4 °C (potting), 0.1 °C (sleeves)
Grid: 1.0, 0.75 and 0.5 mm in plane (5 mm vertical)	With potting, the peak was 214 °C on the coarse grid, 224 °C on our grid and 226 °C on the fine grid. With sleeves, it was 90, 84 and 85 °C. Our values are within about 3 °C of the finest grid.
Sleeve discretization: steady radial conduction through one voxelized 1.5 mm sleeve against the exact cylindrical solution	−4.0 % at 1.0 mm, +8.0 % at 0.75 mm, +6.9 % at 0.5 mm, +2.5 % at 0.375 mm. The error is not monotonic, so we do not claim a direction for the sleeve results.

Table 3. Numerical checks.

5. Sensitivity Analysis

Change From Base Case	Design	Peak Neighbor Wall
Base case	Potting	224 °C
Heat into the failed cell 50 kJ instead of 44.7 kJ	Potting	246 °C
Potting conductivity 1.0 instead of 1.5 W/m·K	Potting	209 °C
Cold plate conductance 250 instead of 500 W/m²K	Potting	226 °C
Failed cell keeps intact-cell conductivity (0.2 / 30 W/m·K)	Potting	129 °C
Base case	Sleeves	84 °C
Heat into the failed cell 50 kJ instead of 44.7 kJ	Sleeves	90 °C
Aerogel conductivity 28 instead of 46 mW/m·K	Sleeves	74 °C
Aerogel conductivity 64 instead of 46 mW/m·K	Sleeves	96 °C
Cold plate conductance 250 instead of 500 W/m²K	Sleeves	89 °C
All three: 50 kJ, 64 mW/m·K and 250 W/m²K	Sleeves	110 °C
Lid touches the cell tops (no potting layer)	Sleeves	128 °C

Table 4. Sensitivities. All runs cover 300 s and every peak falls inside the window.

The model shows clearly which design holds. For each single input change in Table 4, the potting-only neighbor went above 101 °C, and the sleeved neighbor stayed below it unless heat reached the cell tops. With all three unfavorable inputs at once, the sleeved neighbor reached 110 °C, just above 101 °C. So the sleeves have little margin on their own. The intact-cell case keeps most of the failed cell's heat in its core, so we regard it as a lower bound for the potting design; even then the neighbor wall passes T_1 and T_v.

6. Limitations

- The failed cell is near-isothermal; real cells can develop surface hot spots and side-wall breaches.
- Neighbor reaction heat is not modeled; propagation risk is judged by temperature thresholds measured on whole cells.
- Vent gas is represented only as heat deposited uniformly on the lid; real vent jets and ejecta are hotter and more local. Flame, gas flow and electrical effects are not modeled.
- Busbars and cell top caps are not modeled; the jelly roll meets the top potting directly.
- Properties are constant with temperature. Cell conductivities are from 18650 and 26650 measurements; potting properties and cell specific heat are typical values. The aerogel data are for a 5 mm blanket (Pyrogel XTE, maximum use 650 °C) applied to a 1.5 mm sleeve; a battery-grade thin aerogel and a sealed or film-faced sleeve, so that liquid potting cannot wick in, are assumed.

7. Implications for Pack Design

For a potted cylindrical-cell module, thin aerogel sleeves are an effective, low-volume way to break the lateral propagation path that conductive potting creates. They have little margin on their own. The design should treat the top of the module as part of the barrier: duct vent gas away from the lid above neighboring cells, keep insulation between

cell tops and any metal spanning several cells, and check busbar heat paths. A model of this kind is a screening tool to choose the design that goes into abuse testing; it does not replace that testing.

Revision Note

Revision 1 of this paper is withdrawn and superseded by this revision.

References

1. X. Feng, J. Sun, M. Ouyang, F. Wang, X. He, L. Lu, H. Peng, "Characterization of penetration induced thermal runaway propagation process within a large format lithium ion battery module," J. Power Sources 275 (2015) 261-273. doi:10.1016/j.jpowsour.2014.11.017
2. J. Schöberl, S. Ohneseit, S. Schaeffler, D. Förstermann, L. Grahl, A. Jossen, C. Ziebert, M. Lienkamp, "Thermal runaway characterization of cylindrical lithium-ion and sodium-ion batteries with various sizes and energy contents," J. Power Sources 648 (2025) 237240. doi:10.1016/j.jpowsour.2025.237240
3. W. Q. Walker, "Understanding Thermal Runaway Response Variability: Utilizing the Battery Failure Databank to Inform Thermal Model Driven Design," NASA JSC, June 29, 2021. ntrs.nasa.gov/citations/20210017855
4. K. Shah, S. J. Drake, D. A. Wetz, J. K. Ostanek, S. P. Miller, J. M. Heinzel, A. Jain, "An experimentally validated transient thermal model for cylindrical Li-ion cells," J. Power Sources 271 (2014) 262-268, citing S. J. Drake et al., J. Power Sources 252 (2014) 298-304.
5. Aspen Aerogels, Pyrogel XTE Datasheet, Rev. 4.2.
6. M. Feinauer, A. A. Abd-El-Latif, P. Sichler, M. Wohlfahrt-Mehrens, M. Hölzle, T. Waldmann, "Effects of Main Aging Mechanism and State of Charge on the Safety of 21700 Li-Ion Battery Cells with Ni-Rich NMC Cathode," J. Electrochem. Soc. 171 (2024) 110524. doi:10.1149/1945-7111/ad9356

Starro white papers explain our methods and findings. They are not a substitute for certification or abuse testing. Generic published inputs; no client data. © 2026 Starro LLC, Carrollton, Texas.